Electroexcitation of giant resonances in $^{15}N^{\dagger}$

E. J. Ansaldo, J. C. Bergstrom, and R. Yen*
Saskatchewan Accelerator Laboratory, University of Saskatchewan, Saskatoon, Canada S7N OWO
(Received 11 April 1978)

The giant resonance region of ^{15}N has been investigated by means of inelastic electron scattering in a momentum transfer range 0.36–1.25 fm^{-1}. The data show a splitting of the dipole resonance into two main peaks at 22 and 25.5 MeV, with some structure around 20 MeV and strength extending down to 13 MeV. The structure from 19 to 30 MeV correlates well with radiative capture and photodisintegration data and is in qualitative agreement with shell model predictions of the isospin splitting of the giant dipole resonance. The data show considerable spin-flip $E1$ strength, which agrees well with the predictions of the generalized Goldhaber-Teller model. Additional structure found in the energy region from ~ 14 to ~ 19 MeV has been analyzed as a $C2$-$C1$ superposition. The $C2$ strength in the 14–18.5 MeV region exhausts up to 22% of the isoscalar energy-weighted sum rule (Helm model, $J = 3/2$ assumed). The amount of $C2$ strength in the region from 18.5 to 30 MeV is negligible.

[NUCLEAR REACTIONS $^{15}N(e,e')$, $E=52$–193.5 MeV, $\theta=48°$–141°. Enriched gas target. Measured $\sigma(E',\theta)$. Deduced giant resonances differential form factors. Deduced $C1$, $C2$ strength distributions with Helm model. Compared differential $C1$ form factor to shell model calculations. Compared $C2$ strength to energy-weighted sum rule. Compared $E1$ strength to generalized Goldhaber-Teller model.]

I. INTRODUCTION

The giant resonance (GR) region of ^{16}O has been extensively studied both experimentally and theoretically. It therefore seems desirable to extend such work to the adjacent nuclei ^{17}O and ^{15}N. Electron scattering form factors in particular provide a stringent test for particle-hole calculations of the electric dipole strength distribution in the GR region, as exemplified by the recent work of Norum *et al.* on ^{17}O.[1] Moreover, electron scattering experiments can yield information on the electric quadrupole strength distribution which complements the information obtained by capture reactions, as shown by Hotta *et al.*[2] for ^{16}O. (For a review of GR studies by capture reactions see Hanna.[3])

We report here on our inelastic electron scattering study of the GR region of ^{15}N. Although no (γn) or total photoabsorption cross sections have been reported in the literature for ^{15}N, considerable work has already been done by photodisintegration and electrodisintegration and radiative capture techniques. From such work emerged a fairly complete picture of the structure of the giant dipole resonance (GDR) as well as some information on the quadrupole strength distribution. The $^{15}N(\gamma,p)$ cross section to the ground and excited states of ^{14}C has been studied by Denisov *et al.*[4] and more recently by Murphy *et al.*[5] Information on the photodisintegration of ^{15}N through excited states ^{14}N, ^{14}C, and ^{12}C has been obtained by Patrick *et al.*[6] by means of the reactions $^{15}N(\gamma,n\gamma')$, $^{15}N(\gamma,p\gamma')$, and $^{15}N(\gamma,t\gamma')$. The (γ,p_0) cross section was found to exhaust about 9% of the classical dipole sum rule.[4,5] Decay to excited states appears to be important—the cross sections of Ref. 6 accounting for ~20% of the sum rule. The radiative capture reaction $^{14}C(p,\gamma_0)$ to the GDR has been studied by Weller *et al.*[7] and by Harakeh *et al.*[8] The use of polarized protons has allowed Weller *et al.*[7] and Snover *et al.*[9] to estimate the electric quadrupole strength distribution throughout the GR region.

From these results and the present experiment, the GDR of ^{15}N appears to extend from about 14 to 35 MeV excitation energy with peaks at about 15, 17, 19.5, 20.5, 22, and 25.5 MeV. Furthermore, by a comparison of the above data with the cross sections for the reactions $^{14}N(p,\gamma_0)$ (Refs. 8, 10) and $^{13}C(d,\gamma_0)$ (Ref. 11) it has been concluded that the GDR of ^{15}N displays isospin splitting. The region roughly from 24 to 30 MeV excitation appears to be dominated by $T=\frac{3}{2}$ levels, while the region from 10 to 24 MeV is predominantly $T=\frac{1}{2}$. This dipole strength distribution is in qualitative agreement with the shell model calculations of Fraser *et al.*,[12] Harakeh *et al.*,[8] and Albert *et al.*,[13] performed in spaces of 2h-1p configurations with a variety of residual forces. The remarkably high capture cross sections obtained with complex projectiles such as the $^{12}O(t,\gamma_0)$ work of Schaeffer *et al.*,[14] and the $^{13}C(d,\gamma_0)$ and $^{11}B(\alpha,\gamma_0)$ studies of Del Bianco *et al.*[11,15] point to the importance of higher particle-hole configurations in the GR region of ^{15}N. The only reported calculations in an

extended space is that of Weller *et al.*,[7] who included up to 3p-4h excitations in their calculation of $E1$ reduced strengths.

We have measured inelastic scattering cross sections for ^{15}N in the excitation energy region from ~13 to ~40 MeV. The differential form factors at low momentum transfers are compared to the dipole absorption strength calculations mentioned above. The form factors were integrated over selected excitation energy regions and separated into longitudinal and transverse contributions. The electric quadrupole transition strengths were also assessed for the different energy regions under certain assumptions discussed later.

II. EXPERIMENT AND DATA ANALYSIS

The experiment was performed at the Saskatchewan Accelerator Laboratory using the electron scattering facility described by Auer *et al.*[16] The target was the same as that used in previous studies of ^{15}N states.[17,18] It consisted of 99% enriched ^{15}N gas contained at high pressure (~15 atm) in a cylindrical cell identical to that used for a similar study on ^{17}O.[1] Electron scattering spectra were obtained at seventeen energy-angle combinations in the range from 52 to 194 MeV and 60° to 141°, corresponding to a momentum transfer range from 0.36 to 1.24 fm^{-1}. Angular distributions at fixed q were obtained for six values of the momentum transfer; three were measured at three angles and three were obtained at two angles. This allowed us to extract longitudinal and transverse form factors reliably from $q = 0.36$ to 0.97 fm^{-1}, which assisted in determining the $C2$ contribution. The scattered electron spectra were measured continuously from the elastic peak to about 40 MeV excitation in most cases. Data at higher excitation energies were accumulated every few MeV until the scattered electron energy fell below about 30 MeV. For each incident energy and scattering angle the raw experimental data were corrected in the usual manner for spectrometer dispersion and relative detector efficiencies, and combined to give an energy spectrum.[16] Data were also accumulated with an empty target for subtraction purposes, and analyzed in the same way. The results for excitation energies below 15 MeV have been published elsewhere.[18]

The inelastic scattering form factors were obtained in the usual manner by normalizing to the area of the elastic peak and using the known elastic form factor. The elastic peak areas were determined with a peak fitting code and subsequently corrected for radiative and straggling processes.[19] The elastic scattering form factors were taken from the works of Dally *et al.*[20] (0.86 fm$^{-1} < q <$ 2.7 fm^{-1}) and Schütz[21] (0.22 fm$^{-1} < q <$ 0.48 fm^{-1}). Since these experiments do not give consistent charge distribution parameters for the ^{15}N ground state, and since our data span a momentum transfer range overlapping that of both measurements, the experimental form factors in the range $q = 0.3$–1.3 fm^{-1} were jointly fitted using an harmonic oscillator charge distribution. The fit yielded an harmonic oscillator parameter $a = 1.75$ fm, which includes the center of mass correction and the finite size of the proton.

For the analysis of the giant resonance region the procedures described by Norum *et al.* for ^{17}O were followed.[1] The empty target data were multiplied by a suitable scale factor to account for multiple scattering events and subtracted from the ^{15}N spectra. The radiative tail was calculated[19,22] and multiplied by a scale factor before

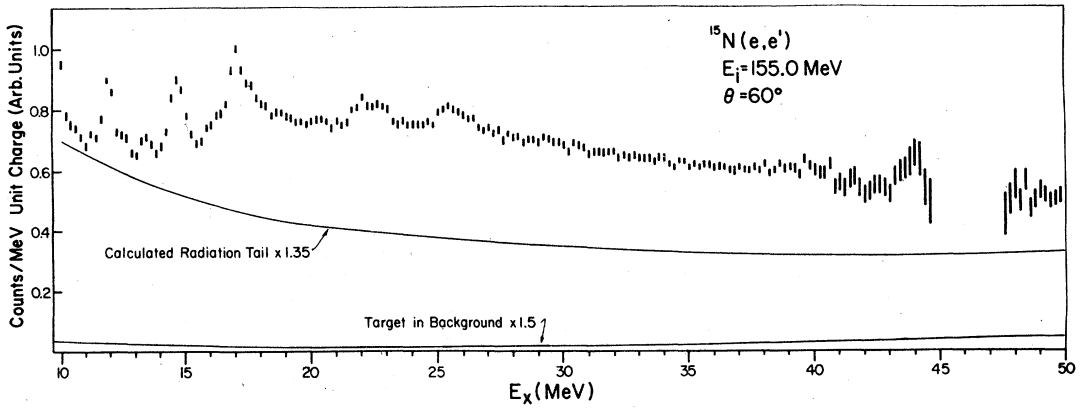

FIG. 1. A sample spectrum showing the contributions due to the elastic peak radiation tail and empty target background. Both backgrounds increase with decreasing q, but the empty target background becomes relatively more important as the momentum transfer decreases.

being subtracted. As in the ^{17}O case, both empty target background and radiation tail scale factors were varied so that (a) together they matched the minima in the data in the region 11–12 MeV excitation and (b) the cross section at excitation energies ≥35 MeV agreed to within 50% with the quasielastic cross section calculated using the DeForest model.[23] The scale factors required varied from 1.2 to 1.5 for the empty target background and were about 1.3 for the radiation tail. A sample spectrum with tail and background is shown in Fig. 1. Both contributions increase considerably with decreasing momentum transfer, with the relative importance of the empty target background increasing the more quickly. Finally, radiative corrections to the continuum above 10 MeV were performed using a uniform bin width of 1 MeV, and affected the cross sections by about 10%. Obviously the background subtraction procedures are a major source of error in this type of experiment. The errors shown in the form factors of the following section were extracted from the spectra in an empirical way, by considering the variations in the experimental areas induced by changes in both background scale factors.

III. RESULTS

Part of the forward-angle data are presented in Fig. 2 as differential form factors defined by

$$|F|^2 = \frac{1}{Z^2\sigma_M}\frac{d^2\sigma}{d\Omega dE_x},$$

where σ_M is the Mott cross section, Z is the nuclear charge, and E_x is the excitation energy. The giant resonance of ^{15}N appears to be highly structured, resembling ^{16}O more than ^{17}O. Several "bumps" are apparent, at excitation energies of 14.7, 17.0, 19.5, 20.50, 22, and 25.5 MeV. The location of such peaks agree well with previous work, but the strength distribution of course is quite different from that of radiative capture experiments.[5,7,8] The peak at 14.7 MeV has already been identified as a $C2$ transition,[18] while the whole structure from ~14 to 18 MeV shows a mixed multipolarity character as discussed below. The other peaks at around 20, 22, and 25.5 MeV are the main components of the giant dipole resonance. The bump at about 17 MeV seems to consist of at least two peaks, one about 400 keV wide and the other somewhat broader, and both are superimposed on the edge of the giant dipole resonance. It was not possible to fit this bump consistently at all momentum transfers by three peak shapes with fixed positions and widths. It is also interesting to note that, as the momentum transfer increases, the strength around 20 MeV excitation decreases and the 22 MeV peak increases relative to the rest of the structure. The q dependence of the area under the 14–18 MeV structure is typical of quadrupole or monopole multipolarity.

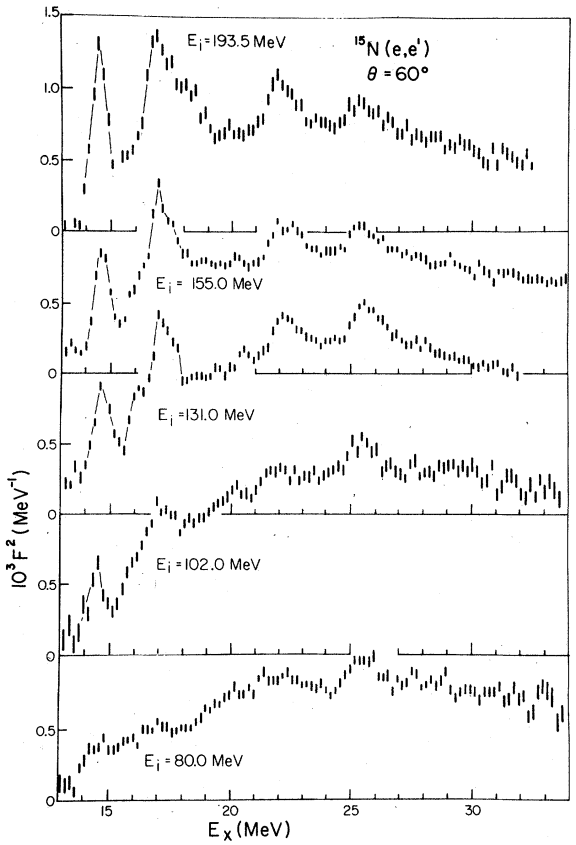

FIG. 2. Electron scattering spectra from ^{15}N in the giant resonance region, presented as differential form factors. All the data taken at 60° are presented here to show qualitatively the evolution of the structure in the GR with increasing momentum transfer.

The backward angle data, as the example of Fig. 3 shows, are much less structured. A similar behavior was found for the ^{16}O (Ref. 2) and ^{13}C (Ref. 22) giant resonances.

Rather than dealing with the finer features of the differential form factors in Figs. 2 and 3, we have chosen to integrate the data over three energy regions: region I, from 14 to 18.5 MeV, region II, from 18.5 to 24 MeV, and region III from 24 to 30 MeV. Regions II and III, from previous experiments and shell-model calculations, are predominantly the $T=\frac{1}{2}$ and $T=\frac{3}{2}$ components, respectively, of the GDR. In region I the previous capture and disintegration experiments are somewhat inconsistent with each other.[8]

The integrated form factors were decomposed into longitudinal and transverse components in the usual plane-wave Born approximation (PWBA)

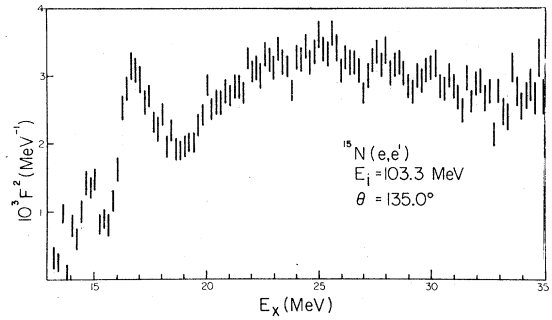

FIG. 3. Differential form factor at 135°. Other backward angle data were obtained at 141° and also show no evidence for strong transverse peaks.

fashion. The momentum transfer dependence of the form factors for region I is shown in Fig. 4. The longitudinal part of the form factor has contributions from more than one multipolarity. Assuming the contributing multipolarities are electric dipole and quadrupole, the form factor was fitted with the Helm model[24] with parameters $R = 2.58$ fm and $g = 1.05$ fm. From the fit shown in Fig. 4(a) the following radiative widths to the ground state were obtained:

$$\Gamma_{\gamma_0}(C1) = (1.1 \pm 0.3) \times 10^3 \text{ eV} \quad (14\text{–}18.5 \text{ MeV}),$$

$$\Gamma_{\gamma_0}(C2) = (12.5 \pm 2.0) \text{ eV},$$

assuming the states responsible are $J^\pi = \frac{3}{2}^+$ for the dipole and $J^\pi = \frac{3}{2}^-$ for the quadrupole component, respectively. Figure 4(b) shows the transverse component of the region I form factor. Its magnitude is about four times larger than that required by Siegert's theorem[24] and the longitudinal form factor of Fig. 4(a).

The integrated form factors for regions II and III were found to be very similar. The sum of the form factors for these two regions (which spans from 18.5 to 30 MeV) is displayed in Fig. 5. The longitudinal form factor of Fig. 5(a) has also been analyzed assuming $C1$ and $C2$ multipolarities and $R = 2.58$ fm, $g = 1.05$ fm in identical fashion to the region I fit of Fig. 4(a). This analysis yields a negligible $C2$ contribution and a $C1$ radiative width to the ground state,

$$\Gamma_{\gamma_0}(C1) = (1.96 \pm 0.04) \times 10^4 \text{ eV} \quad (18.5\text{–}30 \text{ MeV}).$$

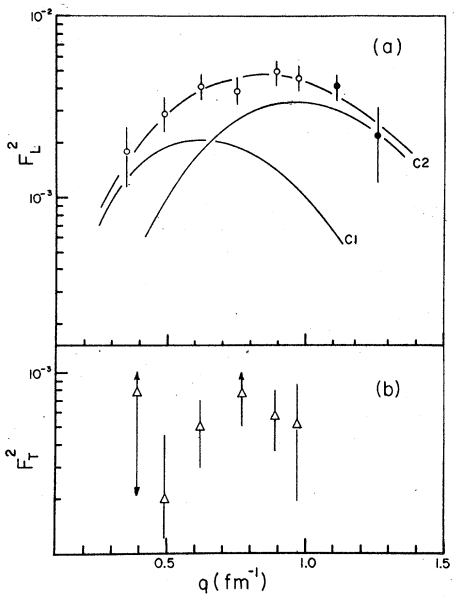

FIG. 4. Integrated longitudinal (a) and transverse (b) form factors for Region I (14–18.5 MeV) as a function of momentum transfer. The solid lines show the average fit and the Helm model $C1$-$C2$ components that yielded the radiative widths quoted in the text. The two points at higher q (dark circles) were obtained from fixed angle spectra by assuming a transverse component extrapolated from Fig. (b). They were not used in the $C1$-$C2$ analysis. The transverse form factor (b) is assigned to the spin-flip $E1$ transitions and as such is considered part of the GDR form factor.

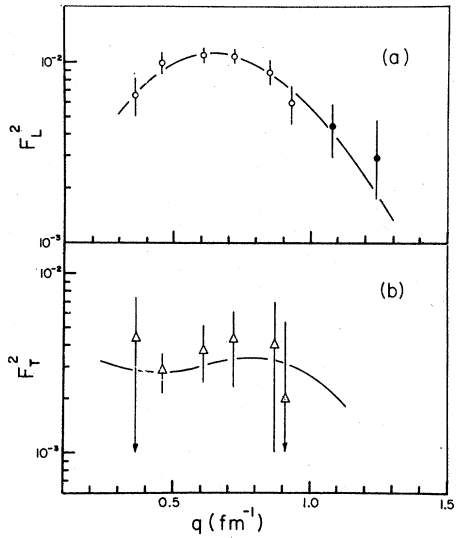

FIG. 5. Integrated form factors for region II plus region III (18.5–30 MeV) as a function of momentum transfer. (a) Longitudinal component. The solid line shows the Helm model fit for a $C1$-$C2$ multipolarity mixture. As discussed in the text, the $C2$ component is negligibly small. Only the data in open circles were used in the fitting. The two points at higher q (dark circles) were obtained from fixed angle spectra by assuming a transverse component extrapolated from (b). They are shown in the plot to demonstrate the consistency of the data at high q with the assumptions made in the analysis. (b) Transverse component. The solid line is the result of using Uberall's generalization of the Goldhaber-Teller model. This calculation is based on the elastic form factor, not a fit to the data points.

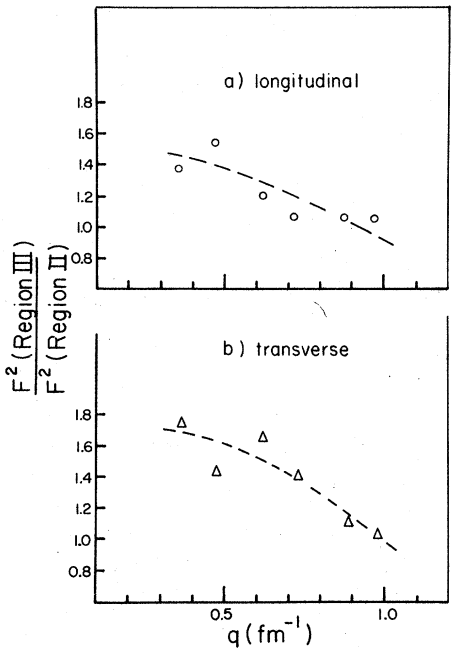

FIG. 6. Ratio of intergrated form factors for region III (24–30 MeV) to region II (18.5–24 MeV) as a function of momentum transfer. The dashed lines were drawn only to guide the eye. The errors were not drawn for the sake of clarity. Statistical errors are about the size of the points, but relative errors due to background subtraction and to longitudinal-transverse decomposition procedure amount typically to 20–25%.

Since this region is overwhelmed by the GDR we can only estimate an upper limit to any $C2$ strength present in our data to be

$$\Gamma_{\gamma_0} < 0.1 \text{ eV}.$$

The transverse form factor expected on the basis of Siegert's theorem and the magnitude of the longitudinal form factor is of the order of 10^{-3}. As shown in Fig. 5(b), the experimental values are around 4×10^{-3}. We have used the Goldhaber-Teller model as generalized by Uberall[25] to estimate the contribution of a $E1$ spin-flip component. The curve shown in Fig. 5(b) is the result of the calculation, based on the experimental form factor. No parameters were adjusted otherwise. Finally, Fig. 6 shows the ratio of experimental form factors of region III to region II as a function of momentum transfer. Both longitudinal and transverse ratios decreasing with increasing q, from a maximum of 1.6 and 1.8, respectively, to about 1.0 at $q \approx 1.0$ fm^{-1}.

IV. DISCUSSION AND CONCLUSIONS

Perhaps the most striking feature displayed by the present work is the distinct splitting of the ^{15}N

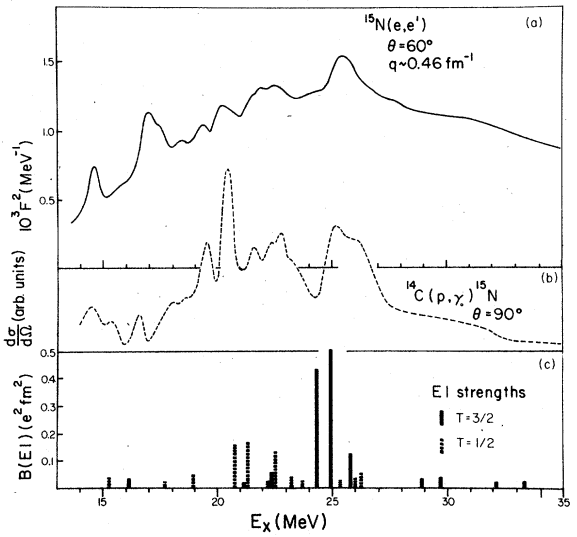

FIG. 7. Comparison of the electron scattering differential form factor ($E_i = 102.0$ MeV, $\theta = 60°$), present work, (a) to (b) the 90° (p,γ) cross section (adapted from Ref. 8) and to (c) the distribution of $E1$ strength at the photon point ($q = E_x/\hbar c$) calculated by Harakeh *et al.* (Table IV of Ref. 8).

giant resonance into two dominant peaks at 25.5 and 22 MeV, whose relative strength decreases with increasing momentum transfer. Evidence that the partition may be isospin splitting of the dipole resonance, with the upper bump consisting mostly of $T = \frac{3}{2}$ states while the lower peak is mainly $T = \frac{1}{2}$, comes from several sources. Those reactions which populate only $T = \frac{1}{2}$ states[10,15] reveal little strength in the 25 MeV region. Theoretical calculations involving 1p-2h (Refs. 8, 12, 13) and 3p-4h (Ref. 7) configurations indicate a tendency for the $T = \frac{3}{2}$ and $T = \frac{1}{2}$ states to separate. By way of example, in Fig. 7 we compare an (e, e') spectrum with the $E1$ distribution calculated by Harakeh *et al.*,[8] and with the ^{14}C$(p, \gamma_0)^{15}$N reaction as measured by these authors. The two strong $T = \frac{3}{2}$ states calculated near 25 MeV have the configuration $[(1p_{3/2}^{-1}1p_{1/2}^{-1})1d_{5/2}]_{1/2^+,3/2^+}$. The 18.5–24.0 MeV region (region II in our analysis) is seen to be dominated by excitation of $T = \frac{1}{2}$ levels, although significant $T = \frac{3}{2}$ admixtures have also been predicted in this region.[7]

The ratio of the form factors of region III (24–30 MeV) and region II (18.5–24 MeV), and its q dependence, *might* be a reflection of isospin splitting. The ratio of $T+1$ to T dipole strengths is predicted to be $1/T$, or 2 for ^{15}N, based on a simple geometrical argument. More detailed considerations[22,26] reduce this ratio, and generally predict a decrease in the ratio of the corresponding form factors with increasing momentum transfer.

TABLE I. Ground state $C2$ radiative widths, and fractions of the energy-weighted sum rule (isoscalar) from this and previous (e,e') work. The $J^\pi=\frac{3}{2}^-$ values in parentheses were assigned arbitrarily to evaluate Γ_{γ_0}.

E_x (MeV)	J^π	Γ_{γ_0} (eV)	$B(C2)$ (e^2 fm^4)	$E_x B(C2)$/EWSR[c]
6.32	$\frac{3}{2}^-$	0.06 ± 0.004[a]	14.80 ± 1.0	0.05
9.16	$\frac{3}{2}^-$	0.10 ± 0.005[a]	3.85 ± 0.2	0.02
9.76	$\frac{5}{2}^-$	0.20 ± 0.05[b]	8.40 ± 2.1	0.05
11.88	$\frac{3}{2}^-$	0.44 ± 0.10[b]	4.60 ± 1	0.03
14–18.5	$(\frac{3}{2}^-)$	12.5 ± 2.0	24.2 ± 4.0	0.22
18.5–30	$(\frac{3}{2}^-)$	<0.10	<0.04	<0.001

[a] Reference 17.
[b] Reference 18.
[c] See A. Bohr and B. R. Mottelson, *Nuclear Structure*, (Benjamin, New York, 1975), Vol. 2, Chap. 6.

The $B(E1)$ values of Ref. 8 (Table IV), when summed, predict a value of ~1.9 for this ratio.

There is structure at 19.5 and 20.5 MeV, which we attribute to dipole transitions which are more evident in the low momentum transfer data. Below 19 MeV any dipole transitions are obscured by other multipolarities. The transverse form factor for the GDR region [Figs. 4(b) and 5(b)] does not vary much with q, and is consistent with Uberall's generalized Goldhaber-Teller model, i.e., there seems to be a considerable amount of spin-flip $E1$ strength throughout. This may be interpreted as evidence that $M1$ strength, if any, is small *vis-à-vis* the $E1$ strength and is not concentrated in any particular energy region of our data.

Under the hypothesis that the only multipoles contributing to the longitudinal form factors are $C1$ and $C2$, we have estimated the electric quadrupole strength distribution within the framework of the Helm model. Present and previous results from (e,e') experiments are shown in Table I as radiative widths to the ground state and fractions of the isoscalar energy weighted sum rule. We have assumed $J^\pi=\frac{3}{2}^-$ for the states in the GR region, in evaluating Γ_{γ_0} $(C2)$. Under such assumptions it was found that region I of our data (14.0–18.5 MeV) shows a comparatively large amount of quadrupole strength, about 22% of the isoscalar EWSR, which is distributed over at least three resonances. The one at 14.7 MeV (~400 keV wide) has been previously studied.[18] As Fig 2 shows, there are at least two resonances at ~17 MeV. These, plus possible $C2$ strength spread throughout region I, account for about 15% of the sum rule. We could not separate the structure at 17 MeV consistently into components. This is perhaps an indication that the dipole strength underlying the quadrupole resonance is also localized. In fact, the (p,γ_0) experiments show peaks at ~14.6, 15.4, 16.6, and 18 MeV,[7,8] while the (α,γ_0) reaction shows resonances at 16.3, 18.9, 21.3 MeV,[15] the (d,γ_0) reaction at 17.7 and 21.9 MeV,[11] and the (t,γ_0) reaction at 16.2, 16.6, 16.7, 17.1, and 17.5 MeV.[14]

It is well known that (e,e') experiments cannot differentiate $C2$ from $C0$ transitions. We have assumed no $C0$ strength to be present, based on the absence of any known $\frac{1}{2}^-$ state in the high ex-

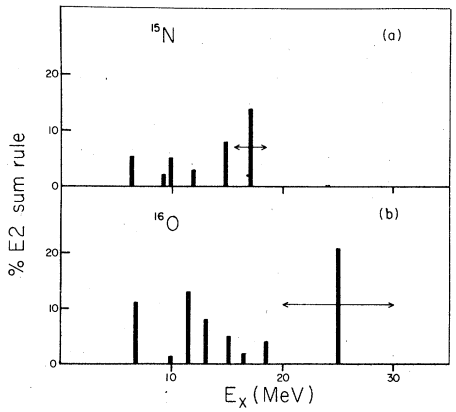

FIG. 8. Comparison of quadrupole strength distribution (as percentage of the isoscalar EWSR) as determined by (e,e'), (a) in ^{15}N, present experiment (see Table I and text for the assumptions made in extracting the $C2$ strength) and (b) in ^{16}O (Table I of Ref. 3). The horizontal arrows indicate the region over which the strength is spread.

citation region of ^{15}N.[27]

In contrast to the region below 18.5 MeV, the 18.5–30 MeV region of our data shows a negligible $C2$ component. It is interesting to compare the quadrupole strength measured here with that in both the ^{16}O case, and ^{15}N as determined by $(\vec{p}, \gamma_0)$ experiments. The quadrupole strength in the 20–30 MeV region of ^{16}O has been found by (e, e') to be ~20% of the sum rule, while the strength in the 15–20 MeV region is about 37%.[3] Therefore, the present experiment indicates a considerable redistribution of quadrupole strength in going from ^{15}N to ^{16}O as shown graphically in Fig. 8. Our upper limit to the $C2$ strength in the GR region is smaller than the 6.8% of the sum rule obtained by Snover *et al.*[9] A similar situation applies in the ^{16}O case, where the $C2$ strength as determined by the $(\vec{p}, \gamma)$ measurements is about 37%,[9] larger than the 20% of the (e, e') experiment.[3] In the 14–19 MeV region unfortunately the $(\vec{p}, \gamma)$ data of Ref. 7 are somewhat ambiguous, and the authors of Ref. 9 report on quadrupole strength only from 19.5 to 27.0 MeV. Therefore, we feel that the present results warrant a careful remeasurement of the 14 → 19 MeV region of ^{15}N by means of the $(\vec{p}, \gamma)$ technique.

We are indebted to H. S. Caplan for his interest in and assistance with the present experiment, and to N. R. Heese for skillful accelerator operation.

---

†Work supported by the National Research Council of Canada.

*Present address: Physics Department, Brooklyn College, CUNY, Brooklyn, New York, 11210.

[1]B. E. Norum, J. C. Bergstrom, and H. S. Caplan, Nucl. Phys. A289, 275 (1977).
[2]A. Hotta, K. Itoh, and T. Saito, Phys. Rev. Lett. 33, 790 (1974); and private communication.
[3]S. S. Hanna, Aust. J. Phys. 29, 511 (1976).
[4]V. P. Denisov, L. A. Kulchitskii, and I. Ya. Chubukov, Yad. Fiz. 14, 889 (1971) [Sov. J. Nucl. Phys. 14, 497 (1972)].
[5]J. J. Murphy, II, Y. M. Shin, and D. M. Skopik, Nucl. Phys. A246, 221 (1975); and private communication.
[6]B. H. Patrick, E. M. Bowey, and E. G. Muirhead, J. Phys. G 2, 751 (1976).
[7]H. R. Weller, R. A. Blue, N. R. Roberson, D. G. Rickel, S. Maripuu, C. P. Cameron, R. D. Ledford, and D. R. Tilley, Phys. Rev. C 13, 922 (1976).
[8]M. H. Harakeh, P. Paul, H. M. Kuan, and E. K. Warburton, Phys. Rev. C 12, 1410 (1975).
[9]K. A. Snover, J. E. Bussoletti, K. Ebisawa, T. A. Trainor, and A. B. McDonald, Phys. Rev. Lett. 37, 273 (1976).
[10]H. M. Kuan, M. Hasinoff, W. S. O'Connell, and S. S. Hanna, Nucl. Phys. A151, 129 (1970).
[11]W. Del Bianco, S. Kundu, and J. C. Kim, Nucl. Phys. A270, 45 (1976).
[12]R. F. Fraser, R. K. Garnsworthy, and B. M. Spicer, Nucl. Phys. A156, 489 (1970).
[13]D. J. Albert, J. George, and H. Uberall, Phys. Rev. C 16, 2452 (1977).
[14]M. Schaeffer, A. Degré, M. Suffert, G. Bonneaud, and I. Linck, Nucl. Phys. A275, 1 (1977).
[15]W. Del Bianco, S. Kundu, and J. Kim, Can. J. Phys. 55, 302 (1977).
[16]I. P. Auer, H. S. Caplan, J. H. Hough, J. C. Bergstrom, F. J. Kline, and R. S. Hicks, Nucl. Instrum. Methods 125, 257 (1975); I. P. Auer and H. S. Caplan, *ibid.* 135, 27 (1976).
[17]J. C. Kim, H. S. Caplan, and I. P. Auer, Phys. Lett. 56B, 442 (1975).
[18]E. J. Ansaldo, J. C. Bergstrom, H. S. Caplan, and R. Yen, Can. J. Phys. 55, 2129 (1977).
[19]J. C. Bergstrom, in MIT Summer Study 1967, MIT Report No. TID-24667 (unpublished), p. 251.
[20]E. B. Dally, M. G. Croissiaux, and B. Schweitz, Phys. Rev. 188, 1590 (1969); Phys. Rev. C 2, 2057 (1970).
[21]W. Schütz, Z. Phys. A273, 69 (1975).
[22]J. C. Bergstrom, H. Crannell, F. J. Kline, J. T. O'Brien, J. W. Lightbody, and S. P. Fivozinsky, Phys. Rev. C 4, 1514 (1971).
[23]T. DeForest, Nucl. Phys. A132, 305 (1969).
[24]H. Uberall, *Electron Scattering from Complex Nuclei* (Academic, New York, 1971), Chap. 6, and references therein.
[25]H. Uberall, Nuovo Cimento 41B, 25 (1966).
[26]B. Goulard and S. Fallieros, Can. J. Phys. 45, 3221 (1967).
[27]F. Ajzenberg-Selove, Nucl. Phys. A268, 117 (1976).